

# EVAPORATION OF LIQUIDS FROM A PARTIALLY FILLED CONTAINER IN A TURBULENT AIR STREAM

K.A. EL Shorbagy

Mech. Eng. Dept., Faculty of Eng., Alex. Univ.  
Alexandria, Egypt.

S.A. El Sayed, M.A. Aziz and M. Emara

Mech. Eng. Dept. Zagazig Univ.  
Zagazig, Egypt.

## ABSTRACT

The process of evaporation of water and toluene from a, cylindrical open-topped, container, subjected to a ducted turbulent air-stream has been experimentally studied. The effect of air stream Reynolds number, liquid level depth and container top edge protrusion on the mass transfer, represented by Sherwood number, has been investigated. The experiments have been conducted at Reynolds number ranging from 37000, to 178000, for a range of depth/diameter ratios and several protrusion heights. Results show that the mass transfer rate for both liquids is substantially affected by both Reynolds number and the cavity depth on top of the liquid surface. The presence of a container edge protrusion relative to the bottom surface of the air duct greatly enhances the evaporation process. An enhancement of Sherwood number (Sh) of as much as 300 % has resulted at a small protrusion ratio (Y/D) of the order 0.2.

## NOMENCLATURE

A	Container cross-sectional area (m <sup>2</sup> )
b	Test section width or height (Figure (1-c))
C	Constant for toluene air system (Ref.14)
C <sub>p</sub>	Constant pressure specific heat (kJ/kg °C)
D	container inner diameter (m)
∅	mass diffusion coefficient (m <sup>2</sup> . s <sup>-1</sup> )
H	cavity depth (m)
h	specific enthalpy (kJ/kg)
h <sub>fg</sub>	latent heat of vaporization (kJ/kg)
K	mass transfer coefficient (m . s <sup>-1</sup> )
M	evaporation rate, (kg/s)
M <sub>a</sub>	Molecular weight of dry air (kg/kg mole)
M <sub>w</sub>	Molecular weight of water vapor (kg/kg mole)
P	Pressure (Pa)
Re	Reynolds number (uD/ν)
Sc	Schmidt number (ν/∅)
Sh	Base surface Sherwood number KD/∅
T	Temperature (K)
u	Mean velocity (m/s)
W	Specific humidity (kg w/kg .a)
Y	container edge protrusion height (m)
Z	Pitot traverse location (Figure (1-c))
μ	Dynamic viscosity (kg/m.s)
ν	Kinematic viscosity (m <sup>2</sup> /s)
φ	Relative humidity %
ρ	density (kg/m <sup>3</sup> )

## Subscripts

a	air (dry)
db	dry bulb
bar	barometric
es	vapor at liquid surface
e∞	vapor in air stream
g	gas
f	liquid
m	mixture
max	maximum
sat	saturated water vapor
w	Water vapor
wb	wet bulb
wv∞	water vapor in air stream

## INTRODUCTION

Evaporation of liquid from surfaces exposed to an air stream has received considerable attention due to its widespread applications in heat exchangers, industrial air-conditioning systems and drying processes.

Although the problem has attracted the attention of researchers for nearly a century, only few works have been conducted on heat and mass transfer by the evaporation of liquids in forced stream of air. El Shorbagy and Khalil [1-2] studied surface evaporation of fresh water and petroleum products from flat plates

in conditions simulating the weather conditions.

The mass transfer characteristics for evaporation from partially filled pans of distilled water, to a stream of air, were determined experimentally by Chuck and Sparrow [3]. The evaporation rates of water from a horizontal water surface into a turbulent stream of hot air or superheated steam at different-stream mass flux and modulated temperatures were experimentally measured by Haji and Chow[4]. The study by Trabold and Obot [5] on evaporation of water by impinging air stream provided predictive equations for the mass transfer coefficient in terms of the flow and geometric conditions. Goldstein et.al [6] investigated mass transfer from a square cylinder and its base plate. The investigation was performed using the so called naphthalene sublimation technique. Their findings revealed that, the general pattern of local mass transfer is somewhat different from that with a circular cavity.

Sparrow and Misterek [7], performed an experimental study on sublimation and evaporation of naphthalene and water at the base surface of a cylindrical cavity. They found that the base surface mass transfer does not decrease monotonically with increasing cavity depth.

An investigation of the evaporation of water from a partially filled cylindrical container to a forced air stream, was conducted by Prata and Sparrow[8]. They inferred that the mass transfer coefficient is affected mainly by Reynolds number and the geometry of the cavity.

Goldstein and Karni[9] studied the effect of wall boundary layer on mass transfer from a cylinder in cross flow. In their work the naphthalene sublimation technique was used to study the effect of three dimensional secondary flows including the horseshoe vortex system on the heat-mass transfer characteristics.

Measurements of local mass transfer of naphthalene sublimation on a surface in the region of the base of a protruding cylinder have been conducted by Goldstein et.al [10]. The study exhibited that, different cylinder heights provided different mass transfer distributions, as higher mass transfer rate occurs with the shorter cylinder when compared to a taller one. The literature survey revealed a general dearth of heat and mass transfer information for open-topped cylindrical containers in the presence of a forced convective flow of air. Moreover, relatively little attention has been given to the case of container protrusion, relative to the air duct bottom surface owing to the complexity of the

flow pattern.

This paper is concerned with mass transfer of evaporating water and toluene from an open-topped cylindrical container to a turbulent air stream, with special attention to the case of container edge protrusion.

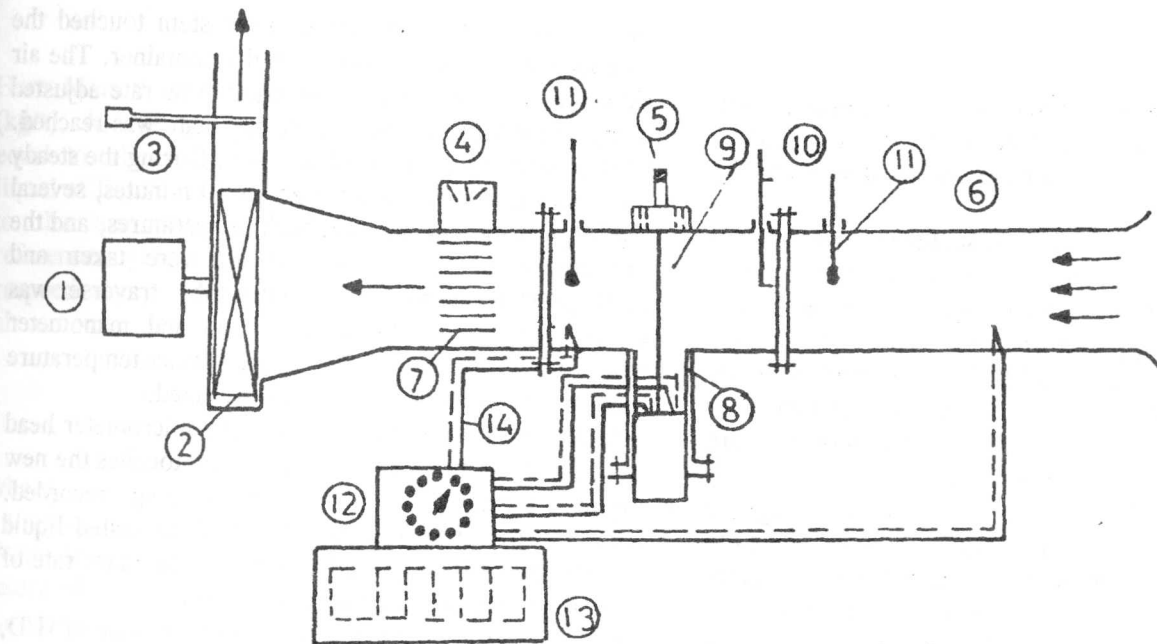
## EXPERIMENTS

### *Experimental Apparatus*

The experiments were conducted in the Thermodynamic Laboratory of Faculty of Engineering, Zagazig University. The experimental facility shown in Figure (1), includes a small aluminium wind tunnel of square section 125 x 125 mm. Through the wind tunnel an air stream is generated and passed over a cylindrical liquid container situated and opened to the bottom lower wall of a perspex working section. This simulates a typical reservoir evaporation in the presence of an air stream.

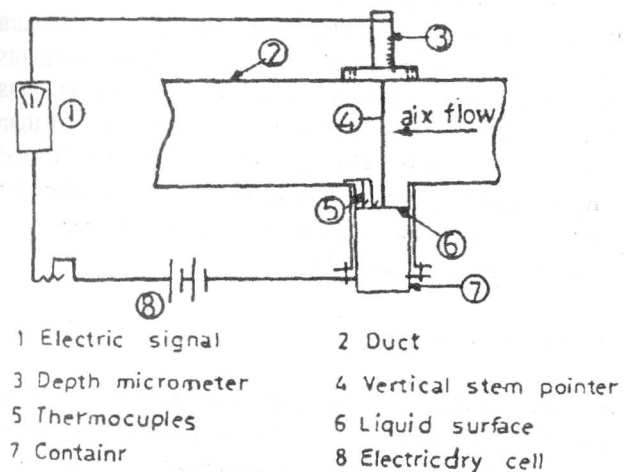
The liquid container is made of aluminium in a multipart assembly of 160 mm length. The inner and outer diameters of the container are 38, and 43 mm, respectively. The evaporating liquid is confined to the lower portion of the assembly, the upper portion being in effect to ensure the cavity depth  $H$  being varied with respect to container inner diameter ( $H/D$ ) in the range from 0.1 to 3. The container surfaces were carefully fabricated to ensure a high degree of smoothness. The perspex test section is 200 mm length of the same cross-section as the wind tunnel, 125 x 125 mm. It has two side flanges for assembly in the main aluminium tunnel. The container opening is located just at the center of the lower wall of the working test section. The system is operated as an open-circuit, in suction mode. Induced air flow enters the apparatus through a bell-mouthed inlet section, flow meter and test section. A transition tunnel leads to a centrifugal fan inlet, regulating valve, and fan discharge. The centrifugal fan, with its inlet to the test section, is driven by 750 W electrical motor. The air velocity through the duct can be regulated by means of a throttle control valve mounted at the exit section of the fan. The total length of the tunnel from the bellmouthed inlet to the test section is 620 mm.

Distilled water and toluene of 99 % purity both at room temperature, were used as the experimental liquids.



- |                        |                           |                               |
|------------------------|---------------------------|-------------------------------|
| 1 Electric motor       | 2 Centrifugal fan         | 3 Throttle valve              |
| 4 Electric signal      | 5 Micrometer head         | 6 Squarer section wind tunnel |
| 7 Honeycomb            | 8 Cylindrical container   | 9 Perspex working section     |
| 10 Pitot tube traverse | 11 Thermometers (db & Wb) | 12 Selecting switch           |
| 13 Digital thermometer | 14 Thermocouple Junctions |                               |

Figure 1. General lay-out of the experimental set-up.



- |                    |                         |
|--------------------|-------------------------|
| 1 Electric signal  | 2 Duct                  |
| 3 Depth micrometer | 4 Vertical stem pointer |
| 5 Thermocouples    | 6 Liquid surface        |
| 7 Containr         | 8 Electricdry cell      |

Figure 1-b. Schematic diagram of the working section showing the experimental container and liquid level measuring instrument.

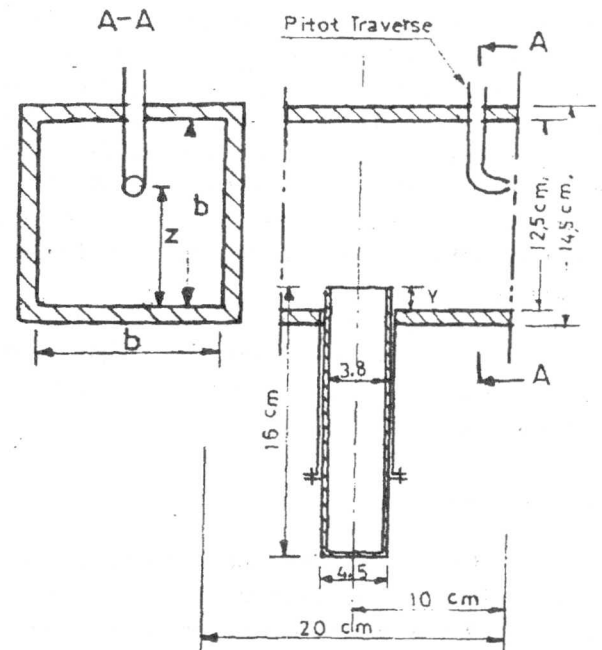


Figure 1-c. The test section with container edge protrusion and pitot traverse locations.

### Measurements

During a test run, liquid and air temperatures as well as air flow rate and evaporated mass of liquid in addition to ambient temperature and relative humidity were to be measured.

As indicated in Figure (1), the surface temperature of evaporating liquid was measured using two thermocouples. The thermocouples were made of 0.25 mm diameter copper-constantan wire chosen for compatibility with water and high output millivolts per °C. The lead outs were connected to a change-over selecting switch. The temperature readouts were displayed on a digital thermometer.

The wet and dry bulb temperatures of air throughout test section were measured by wet and dry bulb mercury in glass thermometers installed both upstream and downstream of the container. The thermometer could be read to within 0.1 °C. Thermocouples were also installed in the duct both upstream and downstream of the container to measure the air dry bulb temperature. Temperature measurements were estimated to be accurate to within 0.74 %

The liquid surface depth (H) was measured by means of a depth micrometer. The micrometer was connected to specially designed electric circuit that gave an electrical signal as the micrometer rod pointer touched the liquid surface, Figure (1-b). The uncertainty in measuring the liquid depth was in the order of 0.04 %. The mass of evaporated liquid could be calculated by estimating the liquid surface depth during two subsequent readings. The velocity distributions across the test section was measured using a Pitot tube connected to an inclined manometer. The uncertainty in velocity measurements is estimated to be in order of 0.6 %. Hence the average velocity and mass flow rate of air were calculated.

The ambient air dry and wet bulb temperatures were measured using a psychrometer. Using the psychrometric chart it was possible to calculate the relative humidity.

### Experimental Procedure

To prepare for test run, the container was filled with the test liquid (distilled water or toluene) to a level consistent with the preselected values of the depth to diameter ratio, ranging from 0.1 to 3.

Then, with the container in place (in the apparatus), the depth micrometer was adjusted so that the tip of the

pointer attached to the micrometer stem touched the free surface of the test liquid in the container. The air flow was initiated and the required flow rate adjusted using the throttle valve until steady state was reached. This usually takes about 15 minutes. During the steady state period, which lasts for about 30 minutes, several readings of the dry and wet bulb temperatures, and the pressure head of the air stream were taken and consequently averaged. A Pitot-tube traverse was carried-out across the duct section and manometer readings were recorded. The liquid surface temperature read-out was also recorded and averaged.

At the end of the testing period the micrometer head was re-adjusted so that the pointer just touches the new liquid surface and micrometer reading recorded. Knowing the change in the depth of the tested liquid and the exact time period of testing, the mass rate of evaporated liquid could be determined.

For the subsequent test run, at another value of H/D, the air flow rate was carefully monitored using the throttle valve and the above-mentioned procedure was repeated. It should however be noted that the recorded value of H/D in all experiments represents the depth to diameter ratio at the beginning of the steady state air flow period. The maximum change in liquid level due to evaporation during this period, in any experiment, was estimated to have not exceeded an effect of 15 % on the recorded H/D value, which is believed to be acceptable in mass transfer applications by evaporation.

In order to study the effect of secondary air stream on the evaporation process, supplementary experiments were performed using water only. In these experiments the upper edge of the container was rather higher than the down duct wall. The top edge protrusion Y was changed during experiments in the range between 3.5 to 9.5 mm. The same above-mentioned procedure of measurements was considered.

### Data Reduction

For both water and toluene evaporation, the mass transfer characteristics at the cavity base are expressed via the mass transfer coefficient K and its dimensionless counterpart, the Sherwood number Sh, respectively defined as:

$$K = (M/A) / (\rho_{cs} \rho_{c \infty}) \quad (1)$$

$$Sh = KD / \mathcal{D} \quad (2)$$

Here  $M$  is the evaporation rate during the data run (kg/s),  $A$ , the cross-sectional area of the container, equal to  $\pi D^2/4$ , and  $\rho_{es}$  the density of evaporating liquid at liquid surface.  $\rho_{es}$  has been found according to the average surface liquid temperature from references [11] and [12] for water and toluene, respectively.  $\rho_{e\infty}$  is vapor density in the approaching air stream.

$$\text{For toluene } \rho_{e\infty} \approx 0 \quad (3)$$

$$\text{For water } \rho_{e\infty} = \phi \rho_{sat} \quad (4)$$

where  $\rho_{sat}$  is the density of saturated water vapor, kg/m<sup>3</sup> and  $\phi$  is the relative humidity in the air stream. From the data collected in conjunction with the saturated water vapor in the air stream  $P_{sat}(T_{db})$ , the barometric pressure  $P_{bar}$ , molecular weight of water vapor  $M_w$  and that of air  $M_a$ , the enthalpies  $h_f$ ,  $h_g$  and  $h_{fg}$ , were calculated. Similarly the known thermodynamic relationships were used to estimate the values of specific humidity corresponding to the dry bulb temperature, ( $W_{db}$ ), the partial pressure of water vapor in the air stream  $P_{wv\infty}$ , and hence the relative humidity  $\phi$ .

To complete the determination of Sherwood number given in Eq. (2), it is required to specify the binary mass diffusion coefficient  $\mathcal{D}$ .

For water vapor-air system,  $\mathcal{D}$  was obtained knowing the values of dynamic viscosity  $\mu$  and Schmidt number ( $Sc$ ) as follows.

$$\rho \mathcal{D}_v = \mu_m / Sc \quad (5)$$

where  $\mu_m$  is the dynamic viscosity of the water vapor-air system. This was calculated by Spalding method described in reference [13]. According to [13], the Schmidt number for water vapor-air system was taken as 0.6.

Concerning toluene binary diffusion coefficient  $\mathcal{D}$ , it was evaluated utilizing the empirical expression employed by Sparrow and Misterek [7] as follows:

$$\mathcal{D}_v = C T^{1.75/P} \quad m^2/s, \quad (6)$$

Where  $C$  is a constant whose value was fixed using data listed in [14], and  $P$  and  $T$  are the pressure and the temperature of the system respectively.

The Sherwood number results will be parameterized by the Reynolds number  $Re$  based on the cavity diameter  $D$  and the mean velocity of air flow in the duct  $u$ .

$$Re = uD/\nu \quad (7)$$

## RESULTS AND DISCUSSION

The evaporating turbulent air stream characteristics are demonstrated by plotting the velocity distribution across the duct for different Reynolds numbers as shown in Figure (2). The data shown in this figure represent a sample result for the traverse at the central meridional plane of the test section. Similar results are obtained at other four planes of the test section. The figure shows that the velocity profile in all cases under consideration is specifically flat all over the test section except for a very thin layer in the close vicinity of the duct walls. The velocity gradient, however, in this layer slightly varies with variation in Reynolds number demonstrating a tendency towards complete turbulence characteristics at higher values of Reynolds number.

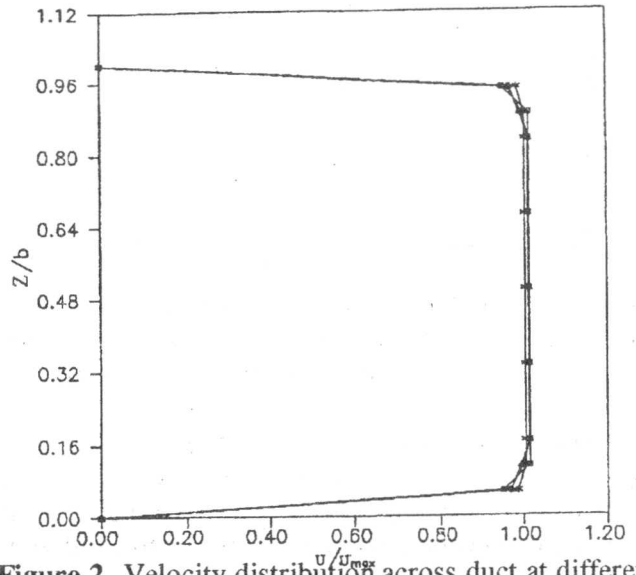


Figure 2. Velocity distribution across duct at different Reynolds numbers.

$$* Re_{(1)} = 37.700 \quad \Delta Re_{(3)} = 144,000$$

$$\diamond Re_{(2)} = 89.000 \quad \bullet Re_{(4)} = 178,000.$$

The mass transfer experimental results are pictured in Figures (3) to (5), in the form of Sherwood number  $Sh$  versus  $H/D$  for different values of Reynolds numbers,



different test liquids and different protrusion ratios, respectively.

Figure (3) demonstrates the variation of Sherwood number with water depth ratio at three different values of Reynolds numbers, namely 37000, 89000 and 144000. From this figure it is clear that the tracing of data curves as  $Sh = f(H/D)$ , for all the considered Reynolds numbers, are practically identical. The mean characteristics of these curves reveal that at constant  $H/D$  the mass transfer rate, as described by Sherwood number ( $Sh$ ), increases with increase in Reynolds number. It can be noticed that the average enhancement of Sherwood number is almost of the same order of increase in Reynolds number.

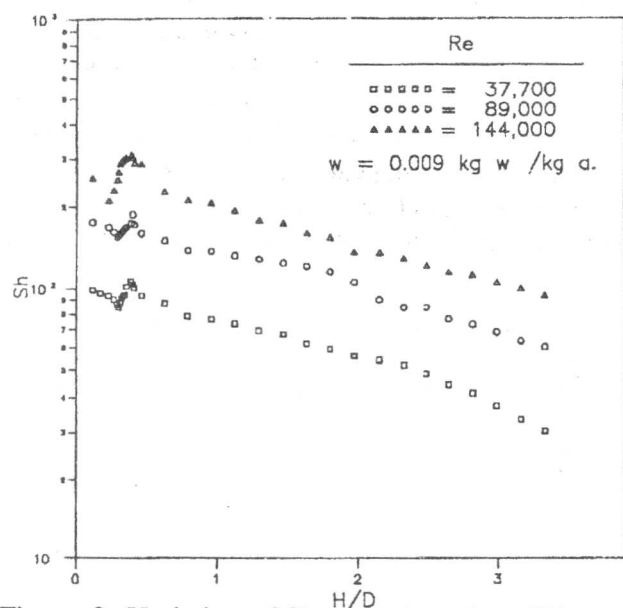


Figure 3. Variation of Sherwood number ( $Sh$ ) versus depth ratio in the container ( $H/D$ ) for water evaporation at constant different Reynolds numbers.

A particular feature of the  $Sh$  vs  $H/D$  is formed by the existence of a local maximum. It was found that, this maximum appears at values of  $H/D$  ranging from 0.3 to 0.34. This phenomenon has been observed with all considered Reynolds numbers. The further increase of  $H/D$  is consistent with a decreasing Sherwood number.

A comparison with the results obtained by Prata and Sparrow [8] on the evaporation of water from a cylindrical container in a similar situation, is shown in Figure (4). The figure shows a similar pattern of variation for the relation  $Sh$  vs  $H/D$ . However, it is clear that higher values of Sherwood number are

obtained by Sparrow et al. Also, the data in the peak region shows a narrow increasing-decreasing crest in the present work results compared to the rather flat peak characteristics of Sparrow et al. Moreover, the peak occurs at a lower value of  $H/D$  in present work. The apparent differences between the present and previous results are believed to be due to different conditions of experiments, particularly difference in air stream humidity in both works since no reference was made by Sparrow et al, concerning its value. It is also depicted that, despite the equality in Reynolds numbers for the present experiments and Prata and Sparrow experiments, the turbulence intensity in the two test rigs could be different due to differences in physical configuration of the rigs. However, no information about turbulence intensity is given in reference [8].

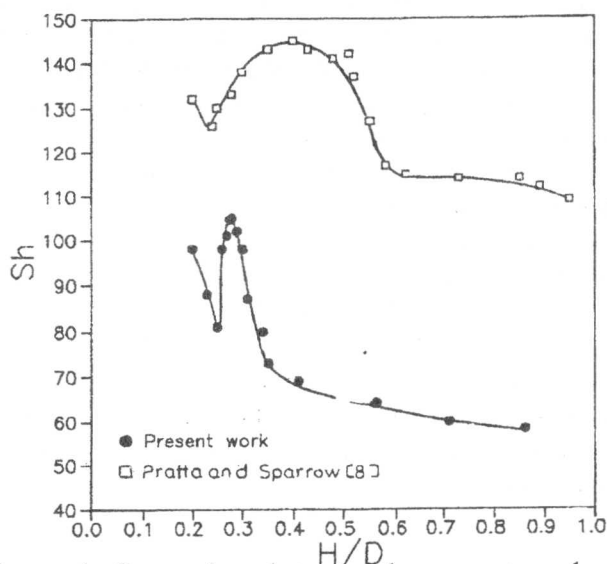


Figure 4. Comparison between the present work and Sparrow work at Reynolds number = 48,000.

Experiments conducted with toluene as the evaporating liquid are illustrated in Figure (5a-b). Results obtained for water evaporation in the same testing conditions are included for the sake of comparison. The overall examination of Figure (5-a) indicates that a similar pattern of variation is obtained with both liquids regarding the relation  $Sh$  versus  $H/D$ . However, substantially higher Sherwood numbers are obtained on evaporating toluene compared with those of water. This is attributed to the smaller binary mass diffusion coefficient  $D$  of toluene compared to the corresponding value for water vapor air system. For example at a temperature of  $17^\circ\text{C}$ , the binary mass

diffusion coefficients for water and toluene are  $1.6 \times 10^{-3}$  and  $8.43 \times 10^{-6} \text{ m}^2/\text{s}$ , respectively. Moreover, the expanded data in Figure (5-b) shows that the toluene results also display a local maximum thereby indicating that the maximum location is not affected by the tested liquid properties.

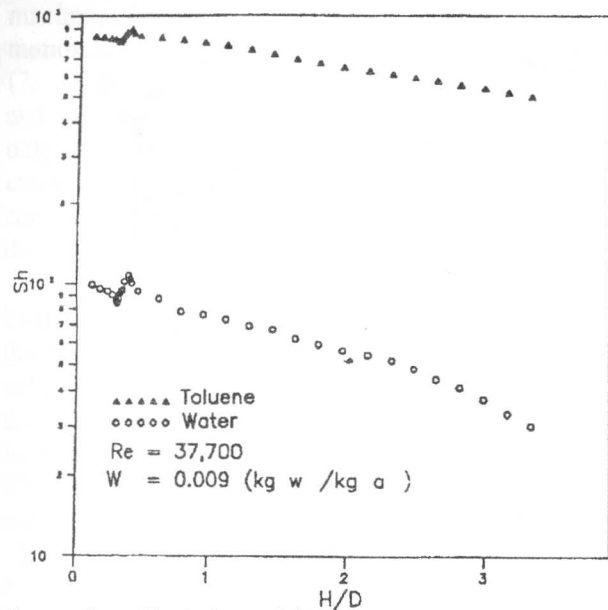


Figure 5-a. Variation of Sh versus H/D for water and toluene at constant Reynolds number and specific humidity.

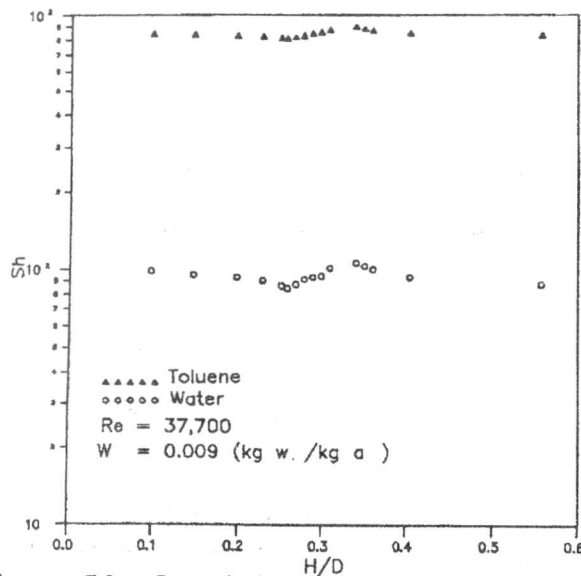


Figure 5-b. Location of the point representing maximum evaporation rates of water and toluene at constant Reynolds number and specific humidity.

The experimental results obtained for evaporating water in the case of container top edge protrusion at constant Reynolds number ( $Re = 89000$ ) are shown in Figure (6) for three values of protrusion height ( $Y = 3.5, 6.5$  and  $9.5 \text{ mm}$ ) respectively.

From this figure, it can be seen that the Sherwood number (Sh) is greatly enhanced by protruding the top edge of the container at any value of Y. The higher the protrusion height the more pronounced is the enhancement of Sherwood number. An increase in maximum Sherwood number of as much as 300 % over the no protrusion value is calculated at  $Y = 9.5 \text{ mm}$ ,  $(Y/D) \approx 0.2$ .

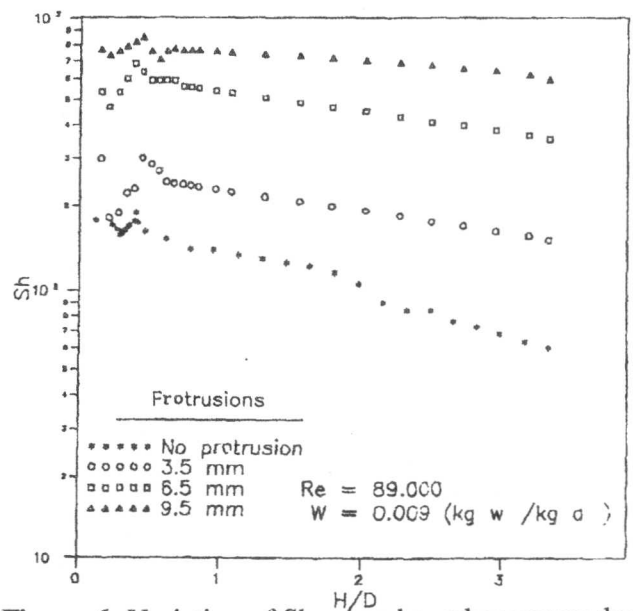


Figure 6. Variation of Sherwood number versus depth ratio for different protrusion heights, at constant Reynolds number and specific humidity for water.

It is worth noting that, the maximum evaporation rates are located in the range of (0.34 - 0.39) for H/D. The corresponding values for zero edge protrusion are (0.3 - 0.34) for H/D. This result finds a remarkable value in practical applications. Thus, in order to achieve relatively high evaporation rates from a deep liquid surface in a container, the container should be elevated to procure reasonable protrusion in the bottom of the evaporating air stream duct.

The characteristic monotonic variation of Sh vs (H/D) may now be considered in view of some notable observations of the liquid surface during evaporation experiments. Schematic representation of the liquid surface in the container is illustrated in

Figure (7), based on the experimental observation, for the cases of low and high Reynolds number and for different H/D situations. When this visualized results are viewed in conjunction with the evaporation characteristics plotted in Figure (3), it could be

conclusively suggested that the process of evaporation of liquid is substantially affected by the state of the air-liquid interface resulting from the aerodynamic reaction at the liquid surface in the container. This may be highlighted as follows:

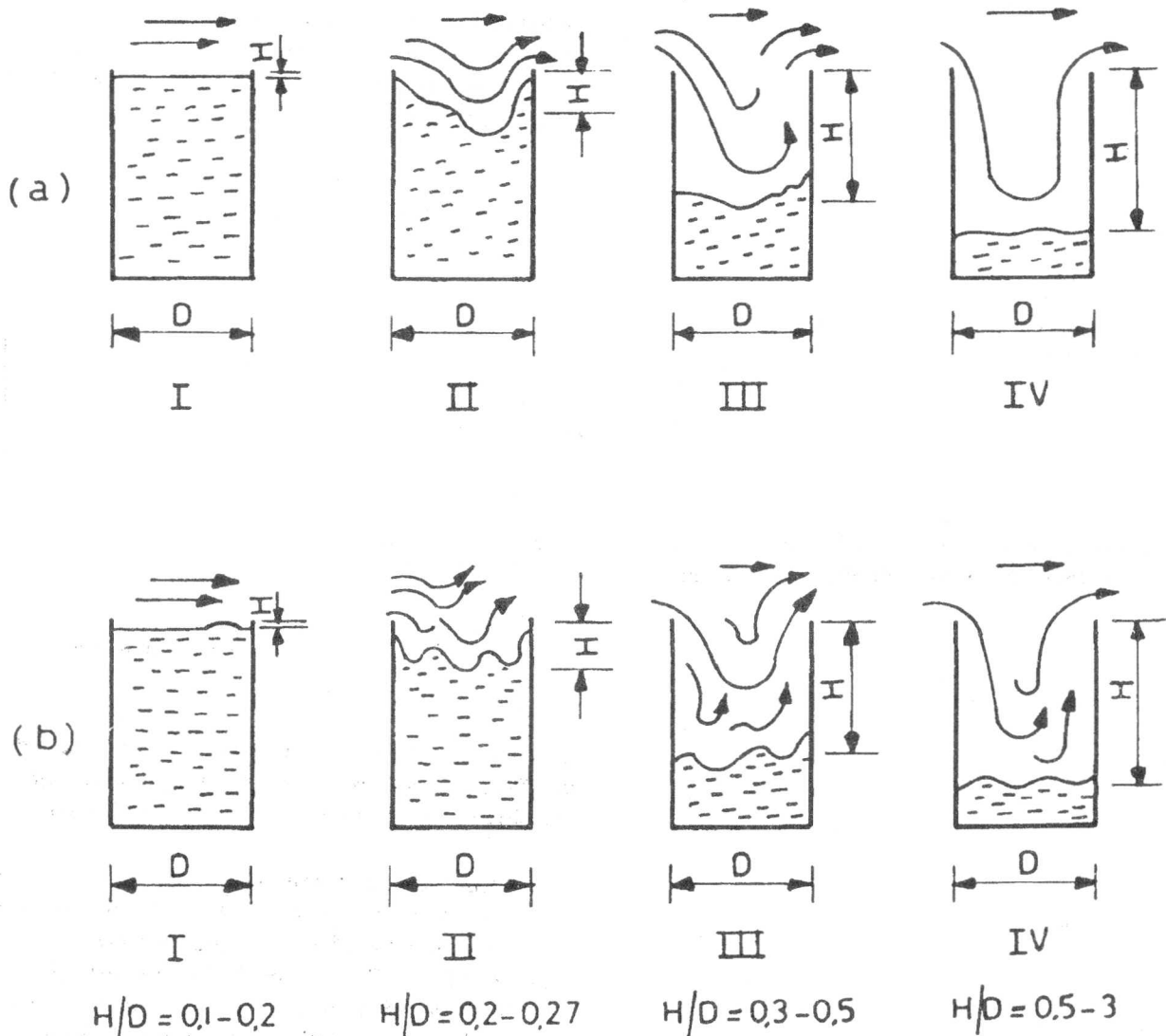


Figure 7. Approximate scheme of the mechanism of evaporation of liquid in stream of air for various H/D  
 a- Low value of Reynolds number. b- High value of Reynolds number.

On increasing H/D from 0.1 to 0.2 an apparent reduction in Sh occurs as can be seen in Figure (3), at any value of Reynolds number. In this case the evaporation of liquid is believed to occur from a surface practically equal to the cross-sectional area of the container as is pictured in Figure (7).

With further increases in H/D from 0.2 to 0.25, the Sherwood number increases vigorously, approaching a maximum value at  $H/D \approx 0.25$ . In this region the air stream circulates inside the container and impinges on the liquid surface as has been demonstrated by Tsou et al, [15]. This leads to the sloshing of liquid strongly,



Figure (7.b.II). Accordingly the interior surface of container walls becomes fully covered by a liquid layer apt for evaporation. So the evaporation surface is substantially developed causing the foreseen increase in the evaporation rate and hence higher values of Sherwood number.

Passing the value of  $H/D$  corresponding to the maximum Sherwood number, the amplitude of slushing motion is observed to decrease as illustrated in Figure (7). In this case weak ripples are eventually formed and the internal surface of the container wall becomes only partially covered with. Accordingly the evaporation surface area is considerably reduced, compared to the aforementioned state, resulting in a decrease in Sherwood number.

The further increase in  $H/D$  is always accompanied by diminishing of liquid sloshing and disappearance of the ripples as can be seen Figure (7). This causes the value of Sherwood number to decrease. In this region the air stream should suffer a relatively long path to be in direct contact with the evaporating liquid surface. This explains the relatively lower values of Sherwood number at high values of  $H/D$ .

It is worth noting that the increase in Sherwood number with Reynolds number as previously reported can be attributed to the tremendous generation of surface ripples resulting from strong slushing of liquid against the container walls. Thus the evaporation surface is substantially increased. This calls to an increase in Sherwood number, refer to Figure (3) in connection with Figure (7).

The effect of container protrusion height can be explained in view of the development of turbulence pattern of air flow due to the container protrusion. The presence of top edge protrusion would lead to the generation of a recirculating stream in the vicinity of the flow in container top. The intensity of turbulence in this region increases with increasing the protrusion height. The length scale of eddies in this stream is also proportional to the protrusion height. The presence of large scale eddies in addition to a persisting reattachment point on top of the liquid surface in the container would undoubtedly lead to a transport situation in which liquid molecules are carried up by a process of diffusion and forced convection into the flowing stream. The presence of a top protrusion, however, would have the effect of a forward facing step which would certainly violate the recirculating region. This effect, increases the intensity of the prevailing large scale (energy containing) eddies, which

in turn increases the mass transport capacity of the flowing air stream. The aerodynamics of the flow over a protruded cavity in a duct, however, lack a fundamental research from both experimental and theoretical view points.

## CONCLUSIONS

The rates of evaporation of distilled water and toluene contained in a partially filled cylindrical container into a forced stream of air, were experimentally measured. The parametric study included the effects of Reynolds number, the depth of liquid, the vertical distance between the surface of the liquid and the top of the container to container diameter ratio  $H/D$  and the ratio of container edge protrusion height to container diameter  $Y/D$ . A summary of the main results is given below.

1. Under all circumstances, the role of the stream velocity in enhancing the evaporation rate is vital and is likely to be the most dominating.
2. The analysis of the heat/mass transfer analogy represented by Sherwood number as a function of ( $H/D$ ) ratio, at a given Reynolds number, indicates, that the maximum Sherwood number occurs in the range  $0.3 < H/D < 0.34$  in the case of zero protrusion height irrespective of the tested liquid. Results, however, indicate that the evaporation rate of toluene is considerably higher than that of water under the same testing conditions.
3. The evaporation process has been proved to be markedly intensified in the case of container edge protrusion. The maximum Sherwood number is shifted to a higher value of  $H/D$  ratio, and located at  $0.34 < H/D < 0.39$ . This finding is believed to have valuable practical applications.

## REFERENCES

- [1] K.A. El Shorbagy and M.F. Khalil "Evaporation of Surface Liquid Droplet in an Air Stream", *Heat and Flow Power System Components*. Pergamon Press, Editor A.M. Rizk, pp 15, 1979.
- [2] K.A. El Shorbagy and M.F. Khalil "Surface Evaporation of Water and Petroleum Products Under Variable Weather Conditions", *J. AMSE* vol, 13, No.1, pp 55-60, 1984.
- [3] W. Chuck. and E.M. Sparrow "Evaporative Mass Transfer in Turbulent Forced Convection Duct

- Flows", I. *J Heat and Mass Transfer*. Vol 30, N2, pp 215-222, 1987.
- [4] M. Haji. and L.C. Chow "Experimental Measurement of Water, Evaporation Rates Into Air and Superheated Steam", I. *J. Heat Transfer* vol. 110, pp 237-242, February 1988.
- [5] T.A. Trabold. and N.T. Obot "Evaporation of Water With Single and Multiple Impinging Air Jets", I. *J. of Heat Transfer* Vol. 113, pp. 696-704, August 1991.
- [6] R.J. Goldstein S.Y. YOO, and M.K. CHUNG "Convective Mass Transfer From a Square Cylinder and its Base Plate", *Int. J. Heat Mass Transfer*, Vol. 33, No. 1, pp 9-18, 1990.
- [7] E.M. Sparrow and D.L. Misterek, "Mass Transfer at the Base of Cylindrical Cavity Recessed in the Floor of a Flat Duct", I. *J. of Heat Transfer*. vol. 108, pp. 853-859, November 1986.
- [8] A.T. Prata and E.M. Sparrow. "Evaporation of Water From a Partially Filled Cylindrical Container to a Forced Convection Air Flow", *Int. J. Heat Mass Transfer*, vol 29, No. 4, pp. 539-547, 1986.
- [9] R.J. Goldstein and J. Karni. "The Effect of a Wall Boundary Layer on Local Mass Transfer From a Cylinder in Cross Flow", *Int. J. of Heat Transfer*, vol. 106, pp. 260-267, May 1984.
- [10] R.J. Goldstein, M.K. Chyu and R.C. Hain "Measurement of Local Mass Transfer on a Surface in the Region of the Base of a Protruding Cylinder With a Computer Controlled Data Acquisition System", *Int. J. Heat Mass Transfer*, vol 28, No. 5, pp 977-985, 1985
- [11] J.H. Keenan, F.G. Keyes, P.G. Hill, and J.G. Moore, *Steam Tables*, John Wiley and sons New York, 1969.
- [12] C.L. Yaws, *Physical Properties. A Guide to the Physical, Thermodynamical and Transport Property Data*, McGraw Hill, New York, 1977.
- [13] D.B. Spalding *Convective Mass Transfer* McGraw Hill., 1963.
- [14] G.A. Lugg. "Diffusion Coefficients of Some Organic and Other Vapors in Air", *Analytical Chem*, vol. 40 pp. 1072-1077, 1968.
- [15] F.K. Tsou, Shih- Jiun Chen, and Win Aung " Starting Flow and Heat Transfer Downstream of a Backward-Facing Step", I. *J. Heat Transfer* vol. 113, pp 583-589, 1991.